

1

2

Supporting Information (SI)

3

4

Structural studies of thyroid peroxidase show the monomer interacting with

5

autoantibodies in thyroid autoimmune disease

6

7

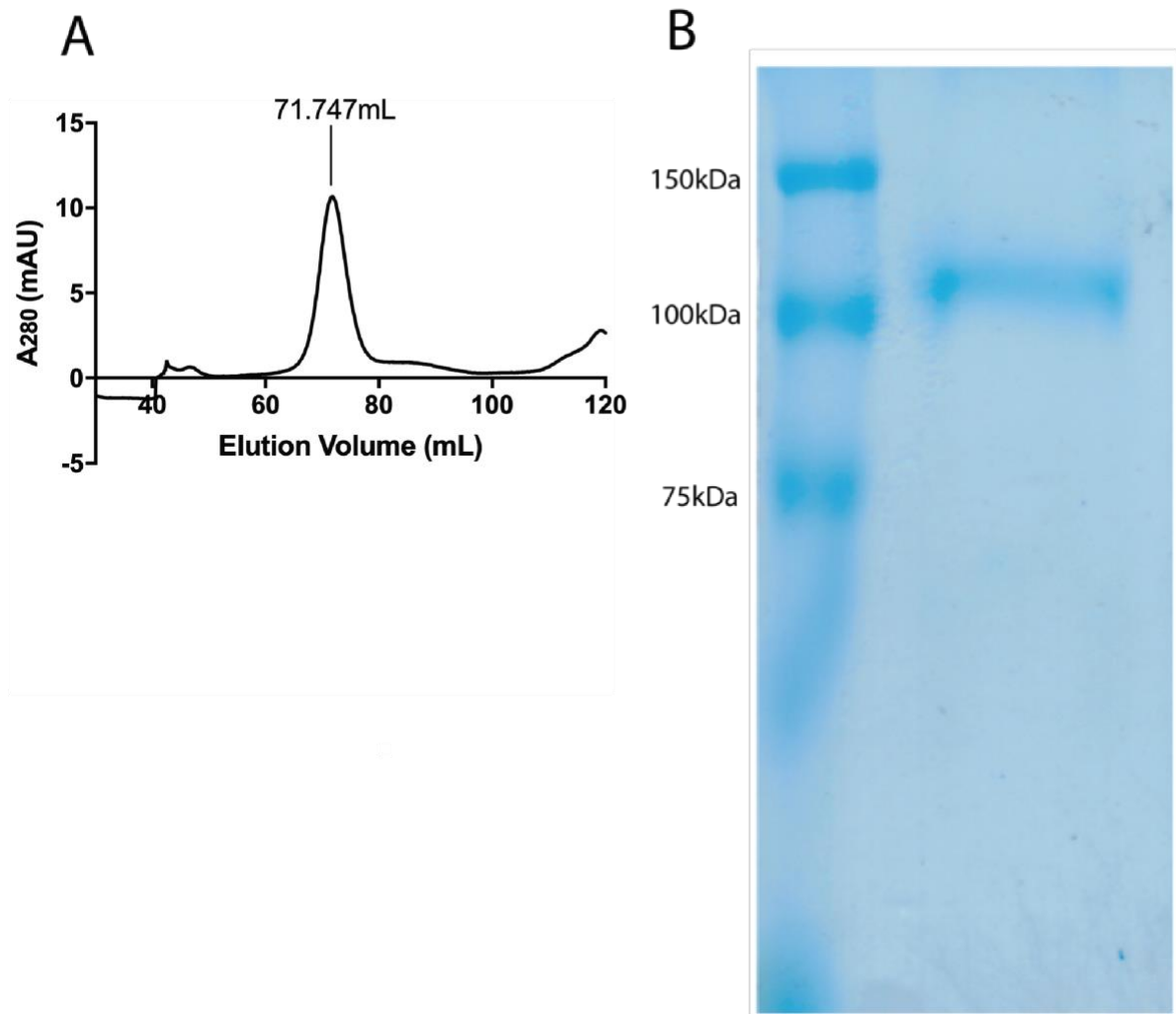
Daniel E. Williams, Sarah N. Le, David E. Hoke, Peter G. Chandler, Monika Gora, Marlena

8

Godlewska, J. Paul Banga and Ashley M. Buckle

9

10



11

12

13 **Figure S1 - Purification of the TPO construct Δ proTPOe-GCN4** (A) A chromatogram from a Superdex
14 S200 16/60 column, showing Δ proTPOe-GCN4 eluting as a single major peak at 71.7mL, consistent
15 with a 110 kDa protein. No other major large species appears to be present. (B) Reducing SDS-PAGE
16 analysis of purified Δ proTPOe-GCN4 shows a major band at ~110 kDa.

17

1	MRALAVLSVT	LVMACTEAFV	PFISRGKELL	WGKPEESRVS	SVLEESKRLV
51	DTAMYATMQR	NLKKRGILSP	AQLLSFSKLP	EPTSGVIARA	AEIMETSIQA
101	MKRKVNLTQ	QSQHPTDALS	EDLLSIIANM	SGCLPYMLPP	KCPNTCLANK
151	YRPITGACNN	RDHPRWGASN	TALARWLPPV	YEDGFSQPRG	WNPGFYNGF
201	PLPPVREVTR	HVIQVSNEVV	TDDDRYSDLL	MAWGQYIDHD	IAFTPQSTSK
251	AAFVGGADCQ	MTCENQNPCF	PIQLPEEARP	AAGTACLPHY	RSSAACGTGD
301	QGALFGNLS	ANPR QQMNGL	TSFLDASTVY	GSSPALERQL	RNWTSAEGLL
351	RVHARLRDSG	RAYLPFVPPR	APAACAPEPG	IPGETRGPCF	LAGDGRASEV
401	PSLTALHTLW	LREHNRLAAA	LKALNAHWSA	DAVYQEARV	VGALHQIITL
451	RDYIPRILGP	EAFQYVGPY	EGYDSTANPT	VSNVFSTAAF	RFGHATIHPL
501	VRRLDASFQE	HPDLPGLWLH	QAFFSPWTL	RGGGLDPLIR	GLLARPAKLQ
551	VQDQLMNEEL	TERLFVLSNS	STLDLASINL	QRGRDHGLPG	YNEWREFCGL
601	PRLETPADLS	TAIASRSVAD	KILDLYKHPD	NIDVWLGGLA	ENFLPRARTG
651	PLFACLIKQ	MKALRDGDF	WWENSHVFTD	AQRRELEKHS	LSRVICDNTG
701	LTRVPMDAFQ	VGKFPEDFES	CDSITGMNLE	AWRETFPQDD	KCGFPESVEN
751	GDFVHCEESG	RRVLVYSCRH	GYELQGREQL	TCTQEGWDFQ	PPLCKDVNEC
801	ADGAHPPCHA	SARCRNTKGG	FQCLCADPYE	LGDDGRTCVD	SGRLPRRMKQ
851	LEDKVEELLS	KNYHLENEVA	RLKKLVGERG	TGSHHHHHHH	H

18

19

20 **Figure S2 – Mass spectrometry analysis of ΔproTPOe-GCN4.** Sequence coverage was reported as 70%

21 with a protein score of 19294, making ΔproTPOe-GCN4 the most abundant species in the sample. Full

22 length TPOe-GCN4 is in black lettering, with detected peptides highlighted in red. Note that residues

23 1 through 108 comprise the signal peptide and propeptide that are not incorporated into full length

24 ΔproTPOe-GCN4, though are included here to demonstrate their successful non-inclusion in our

25 construct.

26

27

```

1 MRALAVLSVT LVMACTEAFF PFISRGKELL WGKPEESRVS SVLEESKRLV
51 DTAMYATMQR NLKKRGILSP AQLLSFSKLP EPTSGVIARA AEIMETSIQA
101 MKRKVNLKTQ QSQHPTDALS EDLLSIANM SGCLPYMLPP KCPNTCLANK
151 YRPITGACNN RDHPRWGASN TALARWLPPV YEDGFSQPRG WNPGFYNGF
201 PLPPVREVTR HVIQVSNEVV TDDDRYSDDL MAWGQYIDHD IAFTPQSTSK
251 AAFGGGADCQ MTCENQNPCF PIQLPEEARP AAGTACLPHY RSSAACGTGD
301 QGALFGNLST ANPRQOMNGL TSFLDASTVY GSSPALERQL RNWTSAEGLL
351 RVHARLRDSG RAYLPFVPPR APAACAPEPG IPGETRGPCF LAGDGRASEV
401 PSLTALHTLW LREHNRLAAA LKALNAHWSA DAVYQEARKV VGALHQIITL
451 RDYIPRILGP EAFQQYVGPY EGYDSTANPT VSNVFSTAAF RFGHATIHPL
501 VRRLDASFQE HPDLPGLWLH QAFFSPWLL RGGGLDPLIR GLLARPAKLQ
551 VQDQLMNEEL TERLFVLSNS STLDLASINL QRGRDHGLPG YNEWREFCGL
601 PRLETPADLS TAIASRSVAD KILDLYKHPD NIDVWLGGLA ENFLPRARTG
651 PLFACLIGKQ MKALRDGDWF WWENSHVFTD AQRRELEKHS LSRVICDNTG
701 LTRVPMDAFQ VGKFPEDFES CDSITGMNLE AWRETFPQDD KCGFPESVEN
751 GDFVHCEESG RRVLVYSCRH GYELQGREQL TCTQEGWDFQ PPLCKDVNEC
801 ADGAHPPCHA SARCRNTKGG FQCLCADPYE LGDDGRTCVD SGRLPRRMKQ
851 LEDKVEELLS KNYHLENEVA RLKKLVGERG TGSHHHHHHH H

```

29

30 **Figure S3 – Mass spectrometry analysis of suspected degraded ΔproTPOe-GCN4 fragment.** Sequence
31 coverage was reported as 63% with a protein score of 8710, making a degraded form of ΔproTPOe-
32 GCN4 the most abundant species in the sample. Full length ΔproTPOe-GCN4 is in black lettering, with
33 detected peptides highlighted in red. Note that residues 1 through 108 comprise the signal peptide
34 and propeptide that are not incorporated into full length ΔproTPOe-GCN4, though are included here
35 to demonstrate their successful non-inclusion in our construct.

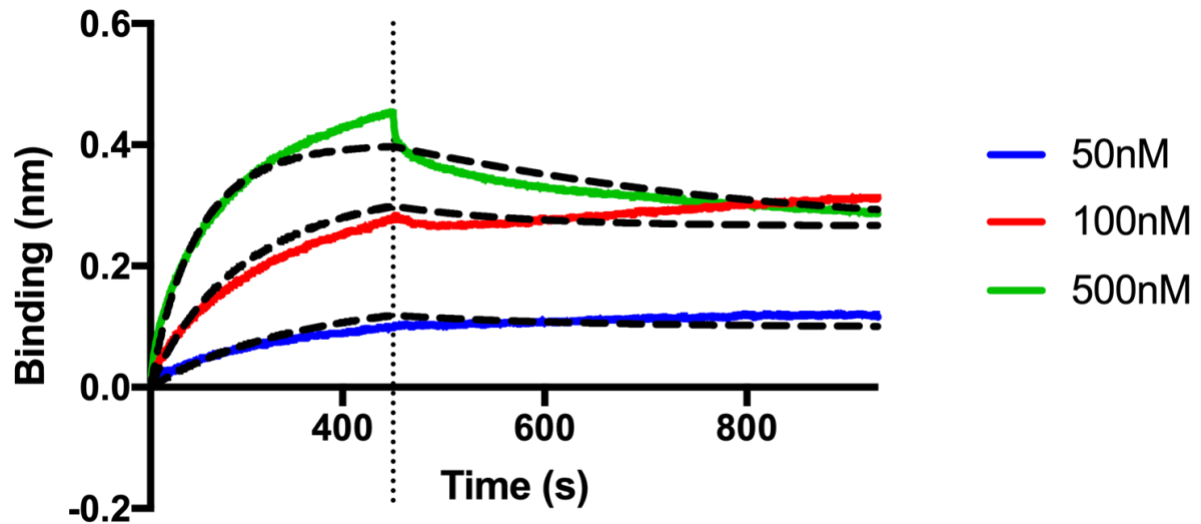
36

37

38

39

40



41

42 **Figure S4 – Bio-layer interferometry (BLI) sensorgram data of Δ proTPOe-8His binding to Fab.**

43 Sensorgram curves according to a TR1.9 Fab concentration range of between 0 and 500 nM.

44 Δ proTPOe-8His is immobilised on the biosensor surface. The data has been normalised against a blank

45 run of buffer (1x PBS, pH 7.4). Vertical line at 450 s represents the end of the association phase. Dotted

46 lines in black represent the fit calculated using a 1:1 binding model with global fitting within the BLItz

47 Pro software. R^2 values for the calculated fit were reported as 0.97. K_D was calculated as 20 nM.

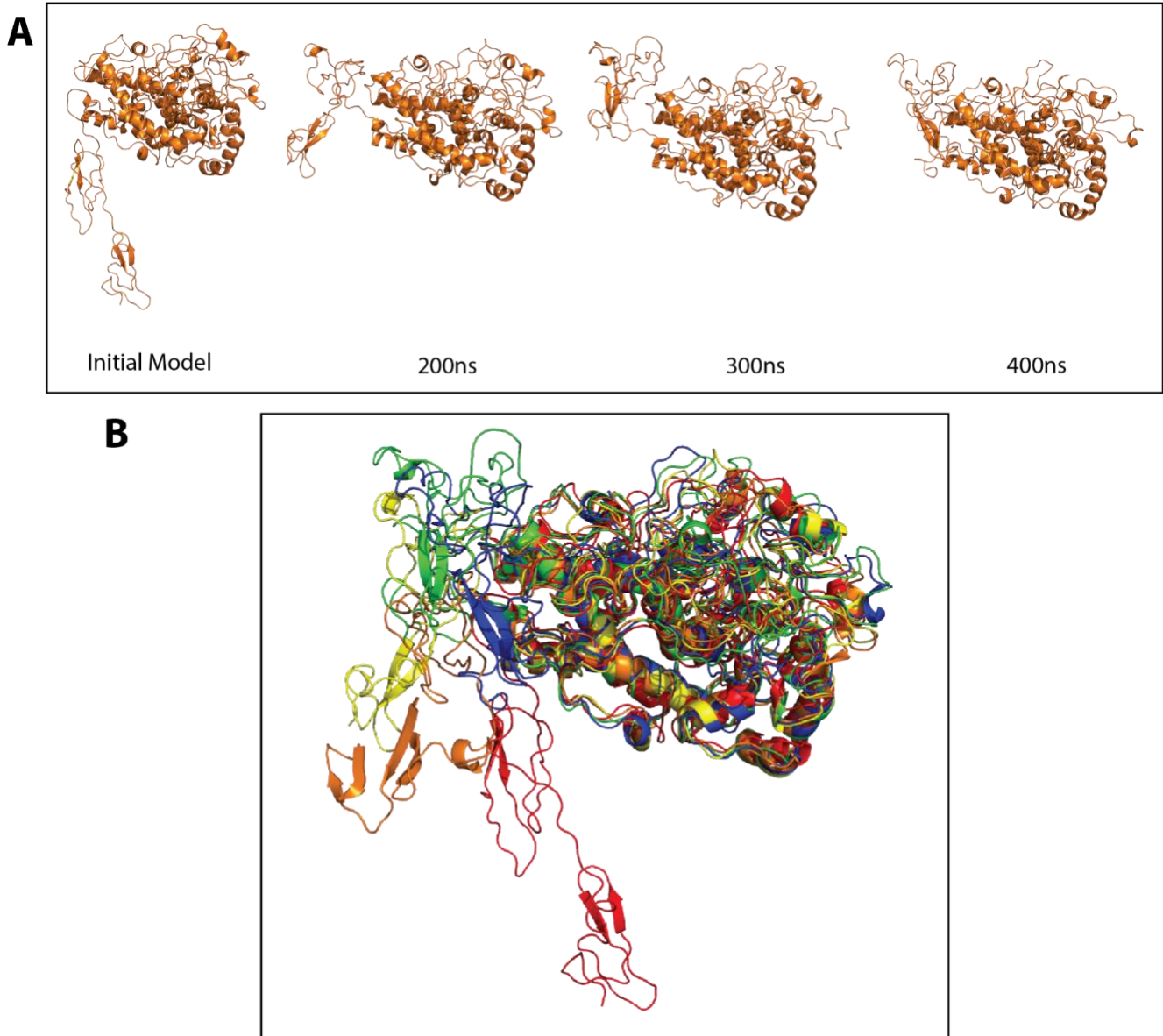
48

49

50

51

52



53

54 **Figure S5 – Snapshots from the *trans* ΔproTPOe MD trajectory show TPO changing conformation**

55 **from extended to more compact structure.** Snapshots from the *trans* ΔproTPOe MD trajectory as

56 presented in Figure 6. **(A)** Representation of the starting model from Le and co-workers ¹, as well as

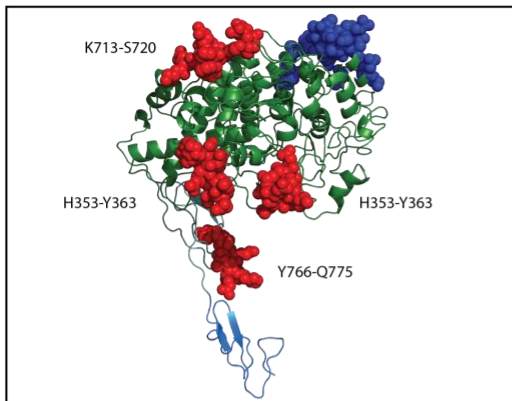
57 *trans* ΔproTPOe after 200, 300 and 400 ns of simulation. **(B)** Structural superpositions of the above

58 snapshots with the starting *trans* ΔproTPOe model in red. Orange indicates *trans* ΔproTPOe after 100

59 ns of simulation, yellow after 200 ns, green after 300 ns and blue after 400 ns.

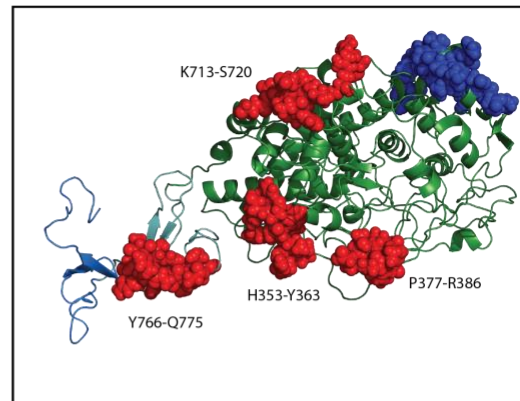
60

A

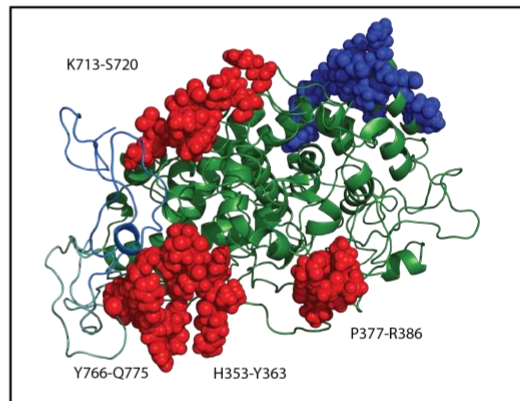
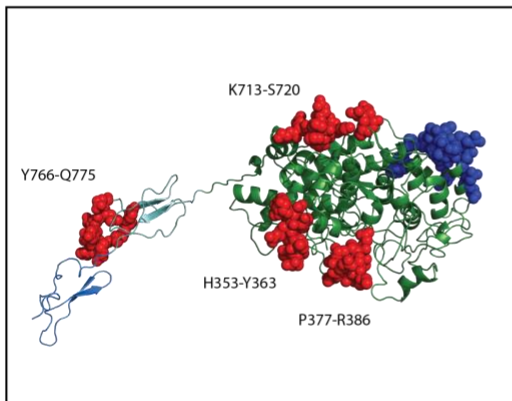


B

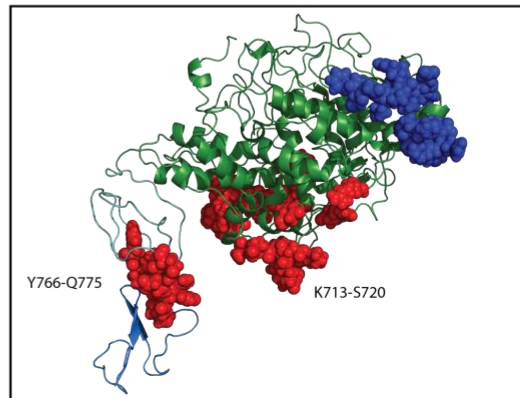
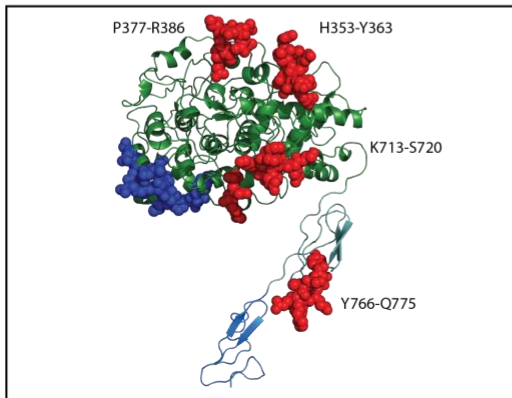
Cis



Extended



Trans



61

62 **Figure S6 – IDRs in context of the MD simulations with starting structures. (A)** TPO models63 (simulation starting structures) with IDRs highlighted. **(B)** Representative structures taken from the64 MD simulations for each of the *trans*, *cis* and *extended* forms of the Δ proTPOe monomer, as in Figure

65 7. IDR-A residues are highlighted by red spheres, and IDR-B residues by blue spheres. The MPO-like

66 domain, CCP-like domain and EGF-like domain are coloured in forest green, light teal and marine blue
 67 respectively (as in Figure 1).

68

69 **Table S1** – Published residues involved in IDRs of TPO

Antibody Involved	Number of Reported Epitopes	Epitopes	Study
IDR-A			
T13	4	H353-Y363, P377-R386, K713-S720, Y766-Q775	2-6
ICA1	1	H353-Y363	2,3
TR1.9	2	K713, K713-S720	2,4,7
126TO10	3	R225, R646, D707	8,9
126TP1	3	R225, R646, D707	8,9
126TP7	1	R225	9
IDR-B			
126TP5	5	D620, D624, K627, D630, F597-E604	8-10
126TP14	5	D620, D624, K627, D630, F597-E604	8-10
131TP7	1	K627	9
SP1.4	1	F597-E604	10
TR1.8	1	T611-V618	10
WR1.7	1	F597-E604	10

70 The epitopes that have been identified as making up the immunodominant regions (IDRs) of TPO,
 71 named IDR-A and IDR-B.

72

73

74

75 **Table S2 – Melting point data of Δ proTPOe-8His in different buffer conditions**

Buffer	pH	T_m (°C)
50 mM HEPES, 250 mM NaCl	8.0	52.3
5 0mM HEPES, 250 mM NaCl	7.0	55.2
50 mM Sodium Phosphate, 250 mM NaCl	6.0	54.7
50 mM Sodium Acetate, 250 mM NaCl	5.5	53.9
50 mM Glycine, 250 mM NaCl	4.0	53.6

76

77

78

79 **Table S3** – Theoretical and calculated Stokes Radii (R_s) of TPO

Reference Dataset	Equation	Stokes Radius (Å)	
		Monomer	Dimer
Globular Folded Proteins	$R_s = (4.75)N^{0.29}$	32.52	39.75
Denatured Unfolded Proteins	$R_s = (2.21)N^{0.57}$	96.93	143.89
Analytical SEC of TPO with no TM domain		51.31	
AUC of Δ proTPOe-GCN4		75.7	91.4
AUC of Δ proTPOe-8His		64.9	77.1
AUC of Δ proTPOe-GCN4 with TR1.9		52.7	66.4
AUC of Δ proTPOe-8His with TR1.9		57.4	N/A

80

81 AUC, analytical ultracentrifugation; SEC, size exclusion chromatography; TM, transmembrane domain.

82

83

84

85

86

87

88

89

90

91

92

93

94

95 **Table S4 – Model Fit Percentages**

Model	Percentage of Molecules within the EM Map
Trans Monomer	73
Cis Monomer	72
Trans Dimer	54
Cis Dimer	59
Trans Monomer with Fab	53
Cis Monomer with Fab	55
Curled Monomer with Fab	58
Curled Monomer with scFv format of TR1.9	73
Trans Monomer with Fab sequentially fit*	68
Cis Monomer with Fab sequentially fit*	70
Trans Dimer with Fab	33
Cis Dimer with Fab	37

96

97 Fit percentages of various TPO models within the electron microscopy (EM) map. Asterisks (*)
 98 indicates configurations where TR 1.9 Fab was fitted into the available space in the envelope without
 99 regard to its epitope's location, rather than in a realistic orientation in which the complementarity
 100 determining regions (CDR) face the published epitope of K713-S720.

101

102

103

104

105

106

107

108 **References**

- 109 1. Le SN, Porebski BT, McCoey J, et al. Modelling of Thyroid Peroxidase Reveals Insights into Its
110 Enzyme Function and Autoantigenicity. *PLoS one*. 2015;10(12):e0142615.
- 111 2. Bresson D, Cerutti M, Devauchelle G, et al. Localization of the discontinuous
112 immunodominant region recognized by human anti-thyroperoxidase autoantibodies in
113 autoimmune thyroid diseases. *The Journal of biological chemistry*. 2003;278(11):9560-9569.
- 114 3. Rebuffat SA, Bresson D, Nguyen B, Peraldi-Roux S. The key residues in the immunodominant
115 region 353-363 of human thyroid peroxidase were identified. *International immunology*.
116 2006;18(7):1091-1099.
- 117 4. Bresson D, Pugniere M, Roquet F, et al. Directed mutagenesis in region 713-720 of human
118 thyroperoxidase assigns 713KFPED717 residues as being involved in the B domain of the
119 discontinuous immunodominant region recognized by human autoantibodies. *The Journal of*
120 *biological chemistry*. 2004;279(37):39058-39067.
- 121 5. Williams DE, Le SN, Godlewska M, Hoke DE, Buckle AM. Thyroid Peroxidase as an
122 Autoantigen in Hashimoto's Disease: Structure, Function, and Antigenicity. *Hormone and*
123 *metabolic research = Hormon- und Stoffwechselforschung = Hormones et metabolisme*.
124 2018;50(12):908-921.
- 125 6. Estienne V, Duthoit C, Blanchin S, et al. Analysis of a conformational B cell epitope of human
126 thyroid peroxidase: identification of a tyrosine residue at a strategic location for
127 immunodominance. *International immunology*. 2002;14(4):359-366.
- 128 7. Guo J, Yan XM, McLachlan SM, Rapoport B. Search for the autoantibody immunodominant
129 region on thyroid peroxidase: epitopic footprinting with a human monoclonal autoantibody
130 locates a facet on the native antigen containing a highly conformational epitope. *Journal of*
131 *immunology (Baltimore, Md : 1950)*. 2001;166(2):1327-1333.
- 132 8. Dubska M, Banga JP, Plochocka D, et al. Structural insights into autoreactive determinants in
133 thyroid peroxidase composed of discontinuous and multiple key contact amino acid residues
134 contributing to epitopes recognized by patients' autoantibodies. *Endocrinology*.
135 2006;147(12):5995-6003.
- 136 9. Gora M, Gardas A, Watson PF, et al. Key residues contributing to dominant conformational
137 autoantigenic epitopes on thyroid peroxidase identified by mutagenesis. *Biochemical and*
138 *biophysical research communications*. 2004;320(3):795-801.
- 139 10. Bresson D, Rebuffat SA, Nguyen B, Banga JP, Gardas A, Peraldi-Roux S. New Insights into the
140 Conformational Dominant Epitopes on Thyroid Peroxidase Recognized by Human
141 Autoantibodies. *Endocrinology*. 2005;146(6):2834-2844.
- 142